

Figure S4: Pictures from petrographic thin sections

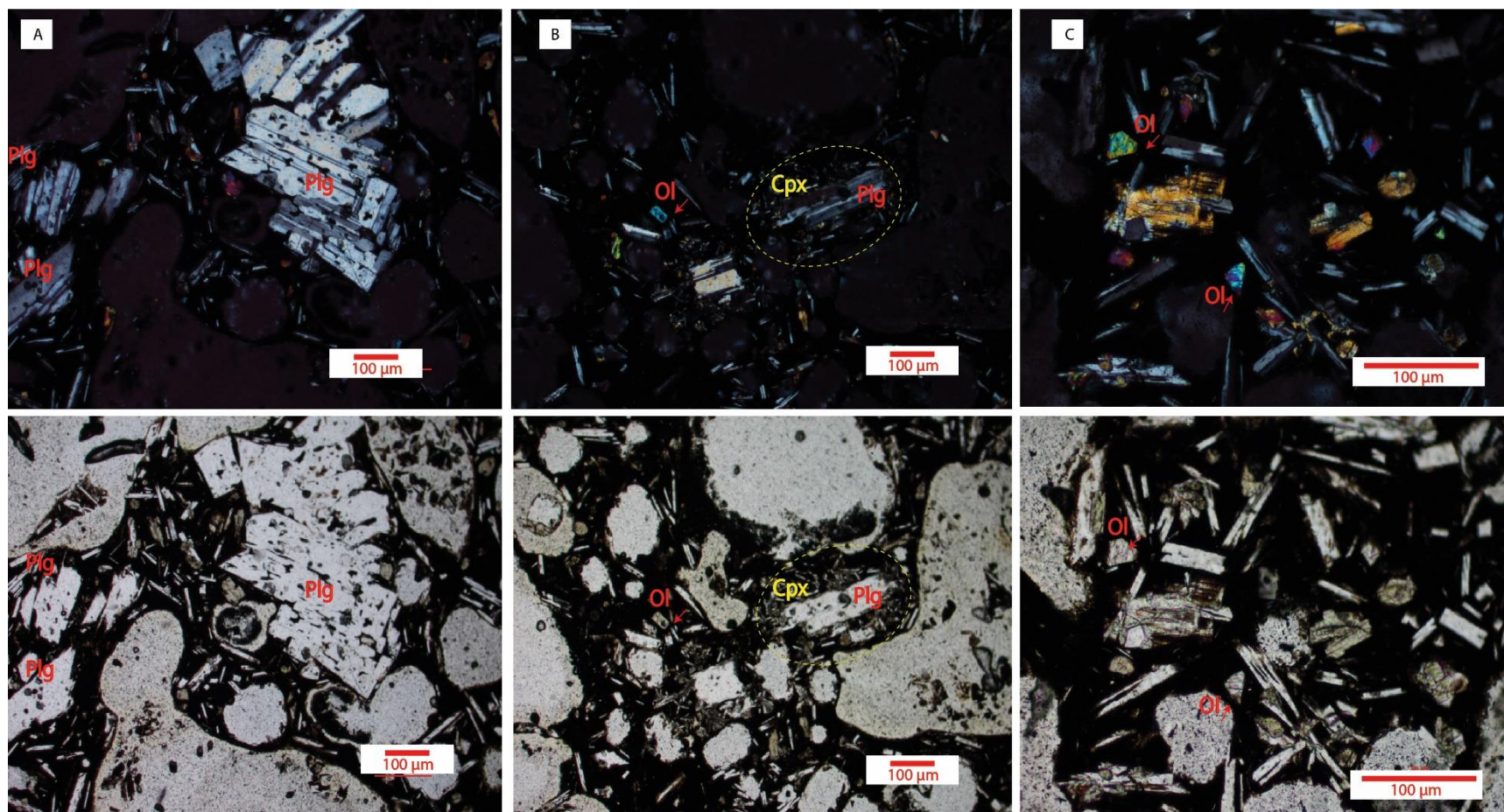


Figure S4a. Photomicrograph superior to crossed Nichols and inferior to parallel Nichols of a transparent section of the fragment HLN2A6A belonging to the eruptive center HLN2A6. (A and B) Crystalline aggregate between olivine and plagioclase, note reentrant edges in plagioclase and olivine. (C) Sieved texture on plagioclase phenocryst.

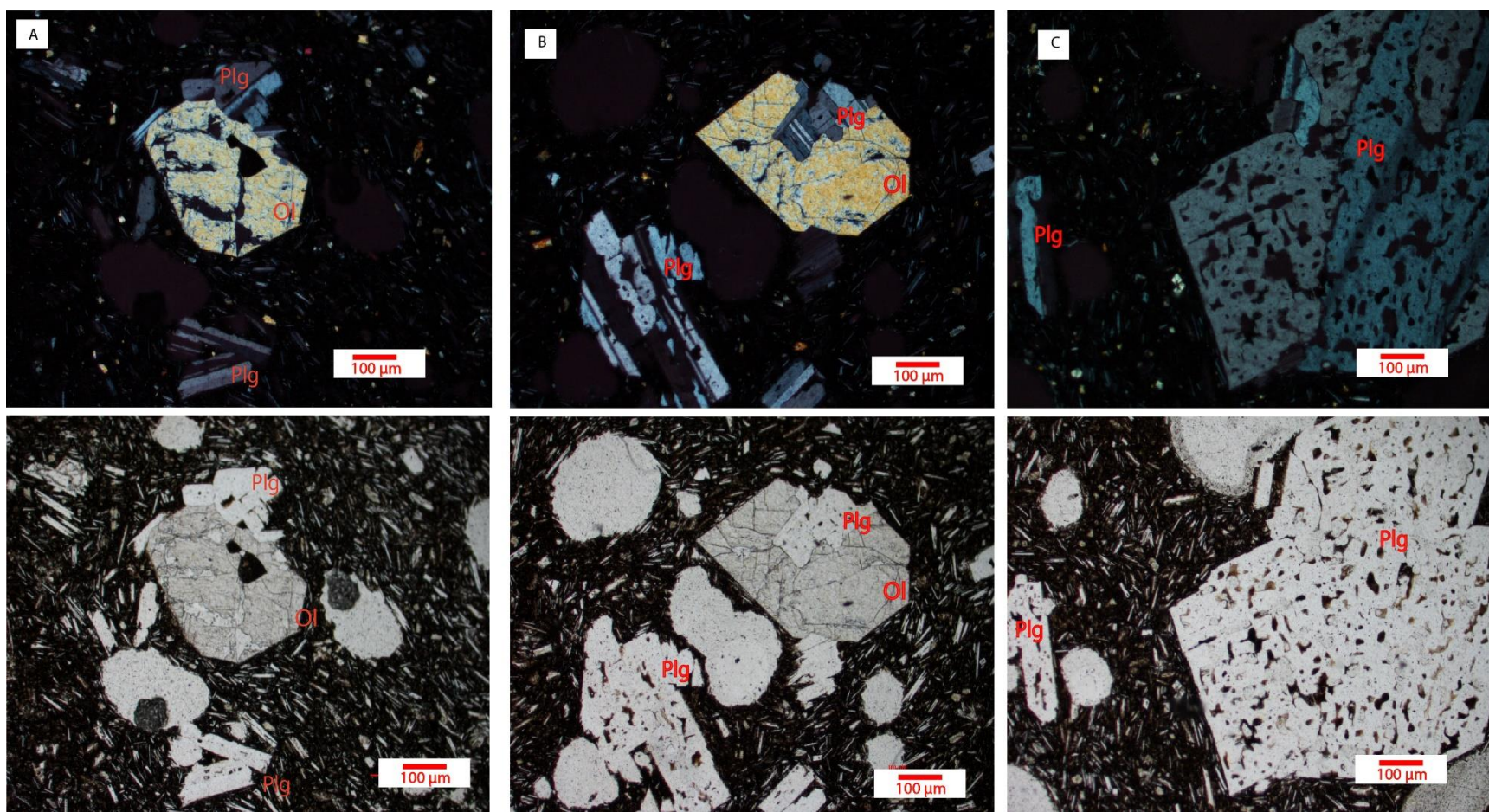


Figure S4b. Photomicrograph superior to crossed Nichols and inferior to parallel Nichols of a transparent section of the fragment HLN2A6F belonging to the eruptive center HLN2A6. (A) Reentrant edges in olivine phenocryst. (B) Crystalline aggregate between phenocrysts of plagioclases and clinopyroxenes. (C) Crystalline aggregate between olivines and plagioclases. Note the low density of visible microlites in the matrix groundmass.

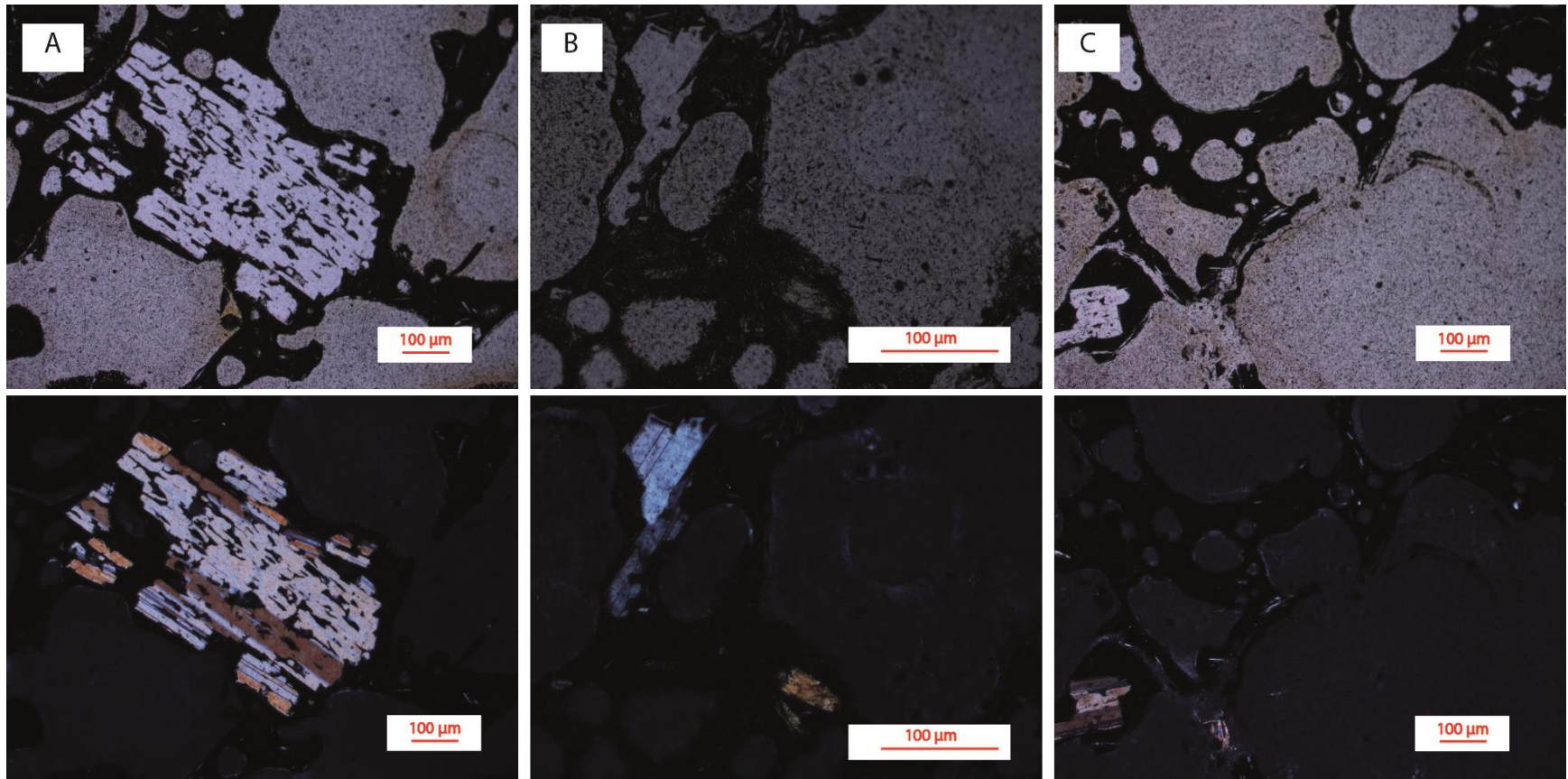


Figure S4c. Photomicrograph superior to parallel Nichols and inferior to crossed Nichols of the vesicular basaltic fragment HLN2A7 belonging to eruptive center HLN2A7. (A) Plagioclase phenocryst showing reentrant edges. (B) Subhedral plagioclase phenocryst with irregular edges that shows reentrant texture, note the abundance of vesicles and the low content of microlites in the matrix groundmass. (C) High vesicular content exhibiting bimodality in vesicular sizes and shapes.

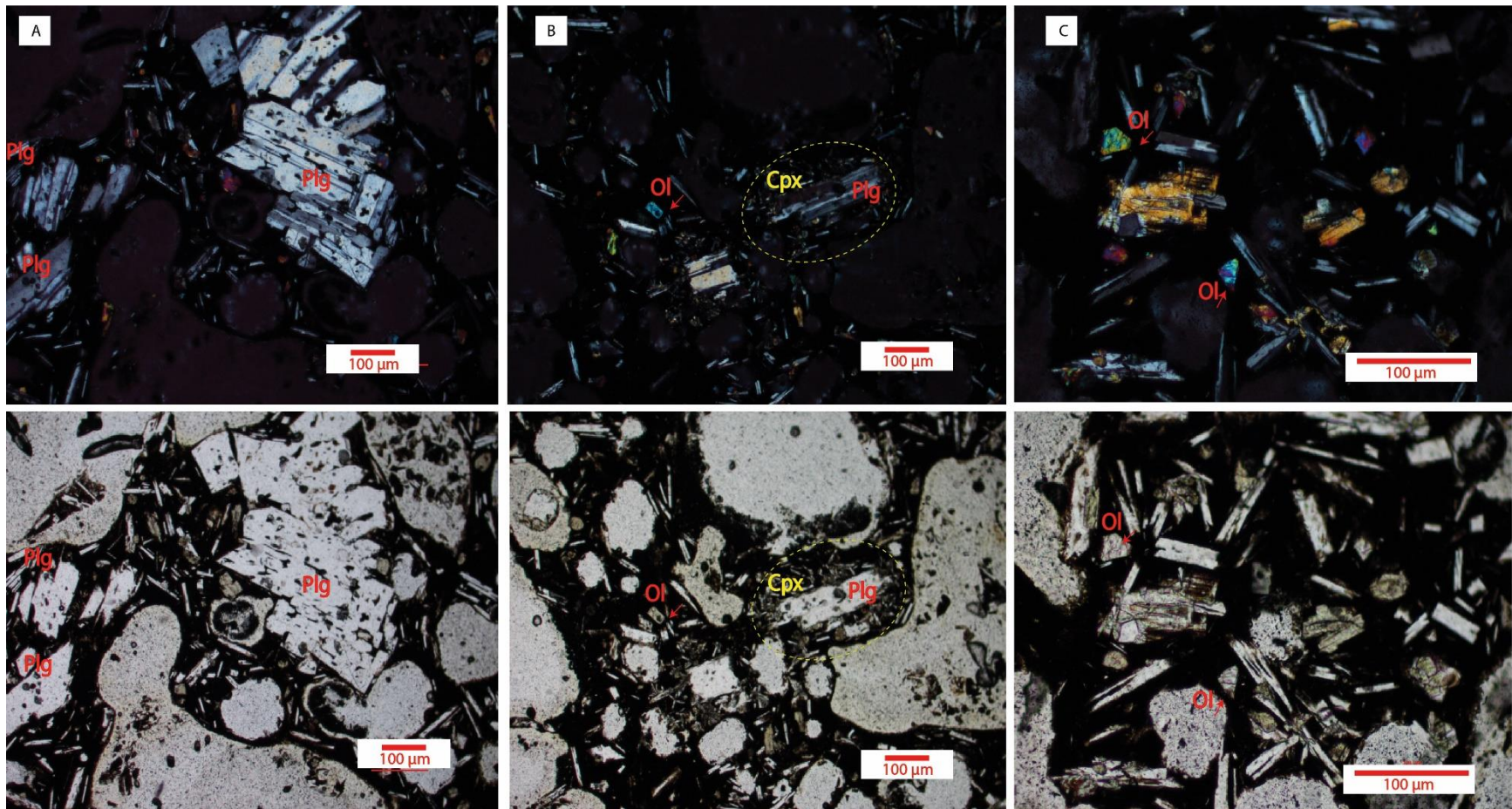


Figure S4d. Photomicrograph superior to crossed Nichols and inferior to parallel Nichols of a transparent section of the fragment HLN2A9 belonging to the eruptive center HLN2A9. (A) Sieved texture on plagioclase phenocryst, (B) Clinopyroxene crystals partially surrounding a plagioclase phenocryst. (C) Crystalline aggregate between olivines and plagioclases.